Journal of Thermal Engineering, Vol. 6, No. 4, pp. 592-603, July, 2020
Yildiz Technical University Press, Istanbul, Turkey

FLOW BOILING HEAT TRANSFER CHARACTERISTICS OF TITANIUM OXIDE/WATER NANOFLUID (TIO_2/DI WATER) IN AN ANNULAR HEAT EXCHANGER

SH. Nakhjavani[1, *], M. A. Abdolhossein zadeh[2]

ABSTRACT

A range of experiments was conducted to measure the heat transfer characteristics of titanium oxide/deionized water nanofluid (NF) inside a steel-made Pyrex annular system. A set of experiments was designed and performed at inlet temperature (IT) of the NF (333 K-363 K), the applied heat flux (AHF) (4.98 kW/m^2 to 112 kW/m^2), 1988 < Re < 13,588 and dispersion concentration of wt.%=0.05 to wt.%=0.15) on the average heat transfer coefficient (HTC) and boiling section's average pressure drop (PD). It was demonstrated that the increase in the volume flow and the AHF can increase the HTC while increasing the weight concentration of the NF, initially increased the HTC such that the maximum enhancement in the HTC was 35.7% at wt.%=0.15 and Re=13500, however, over the time, the HTC of the NF decreased. The reduction in HTC was attributed to the formation of continual sedimentation on the boiling surface after 1000 minutes of the operation. The IT of the NF slightly increased the HTC, which was due to the enhancement in the thermal and physical properties such as thermal conductivity. The maximum enhancement in HTC due to increase of the IT from 333 K to 363 K was 4.2% at wt.%=0.15 and Re=13500. The bubble formation was also found to be a strong function of the applied HF such that with increasing the HF, the rate of the bubble formation increased, which was also the reason behind the augmentation in the HTC at larger AHFs. Also, the PD was augmented due to the increase in the velocity and flow and also weight concentration of NF. The highest value measured for PD was 9 kPa recorded at a weight fraction of 0.15 and Re=13500, which was 28% larger than that of measured for the base fluid. It was also found that a continual fouling layer of nanoparticles (NPs) was formed on the boiling surface, which induced a thermal resistance against the boiling heat transfer. The fouling formation reduced the HTC of the NF such that the maximum reduction in the HTC was 21.6% after 1000 minutes of the operation of the heater.

Keywords: *Annular Heat Exchanger, Flow Boiling, Titanium Oxide/Deionized Water Nanofluid, Thermal Performance, Bubble Formation*

INTRODUCTION

Boiling heat transfer and bubble formation are wonderful phenomena with lots of complex mechanisms and sub-phenomena, which are most of the time unknown and need further research [1, 2]. Generally, boiling occurs on the boundary between the liquid and vapour on which the pressure of liquid equals to its saturation pressure and the temperature is the main external parameter which causes the boiling phenomenon to occur [1, 3-6]. The boiling mechanism is associated with the generation and movement of small bubbles which intensify the heat transfer between the liquid and vapour phases [7, 8]. Hence, boiling heat transfer is a useful mechanism for cooling systems at high temperatures with large heat flux (HF) on the surface [2, 9-12]. Despite its promising thermal performance, some issues need to be addressed such as 1) The thermo-physical properties of the coolants such as heat capacity and thermal conductivity are normally low, which result in a reduction in the system performance. In the conventional low HF boiling systems mixed with natural or forced convective heat transfer, the forced convective HTC is low, which results in the decrease in the cooling and/or heating performance of the system [13-21]. This can affect the design of the heat exchangers (HEXs) as well [22-24].

To overcome the aforementioned challenges, nanofluids (NFs) were developed and introduced by Aragon National Laboratory (ANL) which have better thermal features compared to conventional liquids [6, 25-28]. Since the development of the NF, extensive works were conducted to implement NFs in the HEXs and cooling cycles. Recently, Han et al. [29] found that the presence of the nanoparticles within the conventional coolants can enhance the convective HTC within the HEX. In a study conducted by Ali et al. [30], thermal performance of the titanium oxide/water NF in a car radiator, heat sink and other thermal engineering systems was reviewed and it was shown that NF can promote the thermal conductivity of the liquid. Also, augmentation in the mean pressure drop (PD) was insignificant. Vakili et

This paper was recommended for publication in revised form by Regional Editor Vineet Veer Tyagi
[1]College of Engineering, University of Yazd, Yazd, Iran, Orcid: 0000-0003-1583-1934
[2]School of Engineering, University of South Australia, Australia, Orcid: 0000-0003-0544-4981
[*]E-mail address: shimaa.nakhjavani@gmail.com
Manuscript Received 19 Agust 2018, Accepted 05 December 2018

al. [31] quantified the heat transfer coefficient (HTC) of titania NF and discovered a nonlinear equation between k and weight fraction of the NPs. Also, with increasing the mass flow rate of the flow, the HTC of the NF increased. Azmi et al. [32] assessed a system operating with titania and alumina and demonstrated that at 30ºC, alumina NF requires larger pumping power as it had larger viscosity.

In contrast to the above studies, for the systems working in the two-phase flow, the presence of the nanoparticles can apply a thermal resistance which suppresses the heat transfer mechanisms on the surface. Apart from this issue, there are extensive studies in which it has been shown that HTC can be augmented due to the NPs [7, 9, 33-39]. Hence, more investigations are still required to understand the mechanism of boiling in two-phase systems.

The type of the HEX and more importantly the type of the NPs affect the flow behaviour and thermal engineering in single or two-phase flow [15, 34, 35, 38, 40-44]. Babu et al. [45] showed that hybrid NFs such as a mixture of copper and carbon nanotube can promote the performance of the NF [45]. Huang et al. [46] studied the performance of a hybrid nano-suspension made from carbon nanotube mixed with alumina particles and showed that the HTC of the system can be greatly improved which was largely due to the NPs in the system. Sarafraz et al. [35, 37, 47] conducted a set of experiments on the flow boiling heat transfer of a group of metal oxides including copper oxide, alumina, titanium oxide, silica and noticed that the HTC was a transient parameter, which can be regulated by controlling the thermal fouling resistance. He noticed that the presence of the NPs within the liquid phase reduced the HTC value. The reduction was related to the thermal resistance induced by the deposition layer on the surface. Facing the above literature, in the present study, the thermal performance and the heat transfer characteristics of titanium oxide-deionized water NF inside an annular HEX was investigated. Titanium oxide has some wonderful physical and thermal properties. Hence, here, this material was utilized in a two-phase flow to promote the boiling HTC of the system. A steel made cylindrical surface was used as a boiling surface inside an annular space, which provided conditions for assessing the flow boiling heat transfer of titanium oxide/deionized water. The behaviour of the system was evaluated at variable conditions such as variable velocity, concentration, AHF. The generation of the bubbles inside the base fluid was investigated as well.

Experimental

Test rig

As depicted in Figure 1, the designed system included a piping system for circulating the NF, an annular module as a boiling set up, and all the measurement systems. To continuously circulate the flow, a gear pump with a standard flow accuracy of ±0.7% was used. A hall sensor effect flow meter equipped with an ultrasonic extra sensor with an average accuracy of 0.1% was employed to read the fluid flow. Two transducers were used to measure the pressure before and after the boiling section. Two simple k-type thermocouples were utilised to measure the fluid temperature at two locations close to the pressure transducers. The temperature reading from the thermocouples were inlet and outlet temperatures of the boiling section. To suppress temperature overshoot, the flow was quenched with an R134a thermostat system operating at 298 K. Also, 8 k-type Flexi thermocouples were placed around the circumference of the steel cylinder to symmetrically measure the profile of the temperature. Mean value of the temperature reading was considered as t_{th} referred to as the temperature of the thermocouple. Also, the average of the inlet reading and the outlet reading for the k-type thermocouples was considered as a flow temperature. The main source of thermal energy applied to the cylinder was generated with a boron-nitride rigid heater. Electrical characteristics of the circuit of the element were measured with a multimeter and the power source was a sinusoidal Autotransformer. Figure 2 illustrates the specification of the designed HEX.

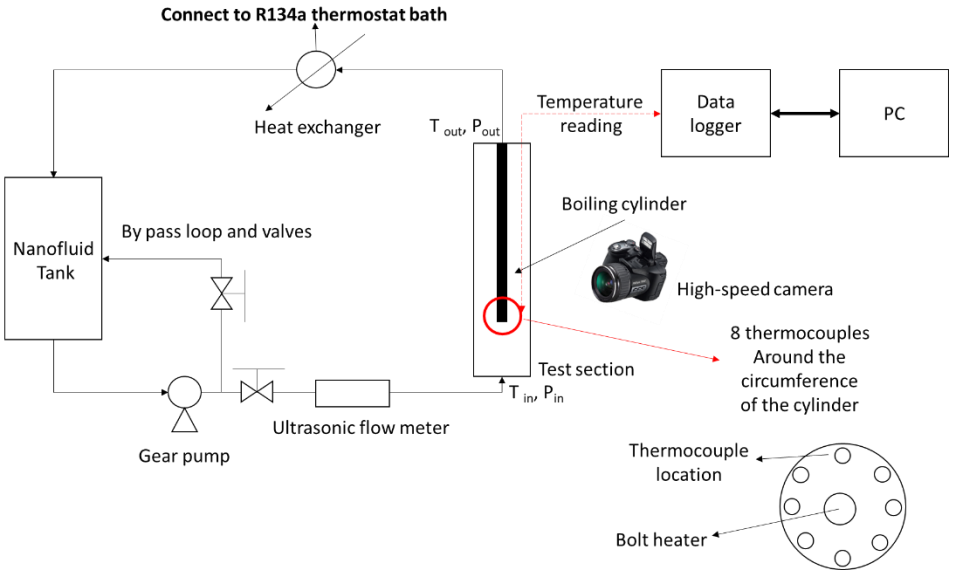

Figure 1. Illustration of the system used for quantifying the HTC of the NF adapted from literature [48].

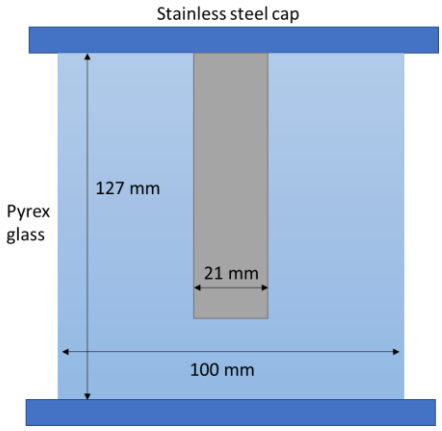

Figure 2. Detailed specifications of the annular HEX similar to the concept developed in the literature [49].

Data reduction

The HTC value was quantified using the following equation:

$$\alpha = \frac{\rho . v . c_p . (T_o - T_{in})}{(T_s - T_f)} \quad (1)$$

Here, ρ is density, v is the liquid volume of NF cooling the surface, c_p is the heat capacity, T is the reading value for the temperature, while two abbreviations of *in-out* stand for measured temperatures before and after the boiling section. "*f*" stands for the film as discussed above and "s" shows the calculated average surface temperature. Notably, the HTC was measured based on the volumetric flow rate, however, for better understanding and to provide a condition for a back-to-back comparison, the mass flow rate was used on the figure legends.

To calculate T_s, equation 2 was used:

$$T_s = T_{th} - q" . \frac{S_{gap}}{k} \quad (2)$$

HF is shown with *q"* and thermal conductivity is shown with *k*, S_{gap} is the small gap created due to the machining between the actual perforation for the thermo-well and the external boiling surface (=0.0017 m). T_{th} is the value of the

temperature reading from each k-type thermocouple close to the surface. The HF was calculated using equation 3 according to the Joule's effect:

$$q" = V.I \tag{3}$$

Using a multimeter, voltage (V) and current (I) of the heater was measured. The calculated value for the uncertainty was obtained with the famous correlation of Moffat as below [50]:

$$\Delta R = \sqrt{(\frac{\partial R}{\partial x_1}\Delta x_1)^2 + (\frac{\partial R}{\partial x_2}\Delta x_2)^2 + (\frac{\partial R}{\partial x_3}\Delta x_3) + ...} \tag{4}$$

Here, ΔR is critical uncertainty of the whole experiments which depends on a different parameter such as x_1, x_2, x_3, ..., x_n, $R = R$ (x_1, x_2, x_3, ..., x_n), and $\Delta x_1, \Delta x_2, \Delta x_3, ...\Delta x_n$ are the values for the uncertainty of each variable. This method is accurate for estimating the instrument errors and has been used in a variety of heat transfer research [11, 47, 51-53]. It was found that the value for the uncertainty in HTC was ~9.8-11.1%, the corresponding uncertainty of HF was ~5.2%, and that of calculated for the PD was ~1%. The density, viscosity, thermal conductivity, heat capacity was computed with the correlations [54] as represented in Table 1.

Table 1. Accurate equations for estimating the properties of the NF [41, 42, 55, 56].

Physical properties	**Correlation***
Density	$\rho_{nf} = \phi\rho_p + (1-\phi)\rho_{bf}$ $\emptyset = \frac{m_p/\rho_p}{m_p/\rho_p + m_{bf}/\rho_{bf}}$
Heat capacity	$C_{p,nf} = (1-\phi).C_{p,bf} + \phi.C_{p,p}$
Viscosity	$\mu_{nf} = A(\frac{1}{T}) - B$ $A = 20587\phi^2 + 15857\phi + 1078.3$ $B = -107.12\phi^2 + 53.548\phi + 2.8715$
Thermal conductivity	$k_{nf} = \frac{k_p + (n-1)k_{bf} - \phi(n-1)(k_{bf} - k_p)}{k_p + (n-1)k_{bf} + \phi(k_{bf} - k_p)} k_{bf} + 5\times10^4 \beta\phi\rho_{bf} C_{pbf}.\Pi$ $\Pi = \sqrt{\frac{\kappa T}{\rho_p d_p}} f(T,\phi)$ $f(\phi,T) = 2.8217\times10^{-2}\phi + 3.917\times10^{-3}(\frac{T}{T_0}) - 3.0669\times10^{-2}\phi - 3.911\times10^{-3}$ For spherical NP: $\beta = 9.881\times(100\phi)^{-0.9446}$, $n = \frac{3}{\varphi}$, φ: *Sphericity of nanopartides* T_0=298K

*nf: nanofluid, bf: base fluid, p: particle, m: mass

Nanofluid preparation

Titanium oxide NPs (40-50 nm with mean reported purity of 99.9%) was received from USnano. To develop the NFs, the following procedure was followed [30]:

1) A quantified mass of NPs was dispersed in the base fluid using an ultrasonic homogenizer (400 Watt, 40 kHz) for 10 minutes. The ultrasonic provided a uniform dispersion of the NPs and cracked any agglomeration and clusters within the NF.

2) to promote longer stability, nonylphenol ethoxylate (NPE) was used at 0.1 vol.%.

To check the stability of NF, time-settlement experiments were designed and performed. It was seen that the sonication guaranteed two-week stability of the NFs within the mass concentrations of 0.05-0.15%. NFs cannot be prepared at higher concentrations because the rate of the sedimentation was not controllable and NFs were unstable at wt.% >0.15.

RESULTS AND DISCUSSION

Heat flux

In Figure 3, the Variation of the HTC with the AHF is illustrated. As perceived, with increasing the HF, the HTC increased. At wt.% of 0.05, at HF 13 kW/m^2, the HTC was ~1230 W/m^2. K (in forced convective regime), while at HF 110 kW/m^2, the HTC reached ~6640 W/m^2. K (in nucleate boiling regime). Bubbles formed on the heating surface are the main cause of the augmentation in the value of the HTC. Such bubbles can also make changes in the flow regime and increase the interaction between layers of the fluid. Also, there are two general mechanisms including forced convective and boiling heat transfer. On a boundary zone, the first layer of liquid is evaporated and form a very small bubble which normally cannot be seen without visualization equipment. This is the point of separation for both heat transfer mechanisms, which is called the Onset of Nucleate Boiling. The heat transfer region before this zone was the forced convective with low HTC value and the heat transfer domain after the point was nucleate boiling with high HTC. The HTC was larger in the nucleate region because of the presence of the bubbles which made a local turbulent regime close to the hot surface, which enhanced the HTC. Also, the micro-convective streams induced by the bubble movements contributed to the enhancement in the HTC. These nano-mechanisms intensified the average value of HTC. Also, the presence of the NPs further intensified the Brownian motion and thermo-phoresis phenomena and also thermal conductivity as well. The maximum HTC was 8710 W/m^2. K measured at the largest HF and for wt.%=0.15. Notably, with increasing the mass concentrations of the NF, the HTC increased. This phenomenon can be attributed to the intensification of the Brownian motion as well. This was because, at a higher mass fraction of NPs, more NPs were available around the hot surface, hence thermal conductivity increases around the surface and better thermal transport occurred.

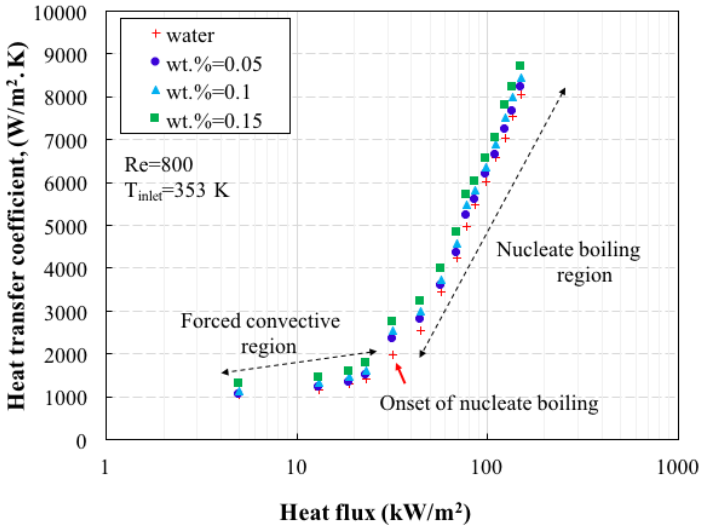

Figure 3. Variation of the mean value of the HTC with the AHF value at different concentration profile of the NPs.

Fluid flow

In Figure 4, HTC variation with the change in the flow is depicted. As perceived, with increasing the Reynolds number, the HTC increased and this behaviour was seen for all NFs and concentrations. The largest recorded enhancement was ~35% (concerning base fluid) and at in the Re > 3500 where the fluid is completely turbulent and at wt.% of 0.15 and Re= ~13500 [57].

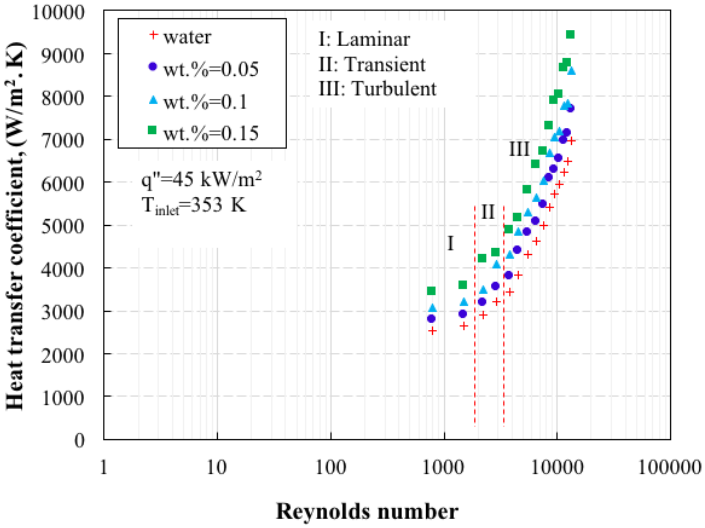

Figure 4. Dependence of the quantified HTC value on the flow rate of the NF.

The inlet temperature of nanofluid

In Figure 5, change in the HTC value with Reynolds number and also the inlet temperature (IT) of the fluid is depicted. As perceived, with increasing the IT, the HTC is augmented slightly. As seen, for a Reynolds number such as 2900 and wt.%=0.15, the HTC at 60 ºC (333 K) is 1788 W/m^2. K, while it reached 1984 W/m^2. K, increasing by ~10.9% at the IT of 90ºC (363 K) and for the same Reynolds number. This can be attributed to the enhancement in thermal conductivity. However, the influence of IT can also slightly increase the Brownian motion. This micro-scale mechanism intensified the thermal transport between the solid NPs and also the bulk of the base fluid. Notably, at a high IT, bubbles formed in a short time and the interactions between the bubbles were more effective in comparison with a lower IT. Hence, the IT of the NF had a slight influence on the HTC. The maximum enhancement in the HTC was recorded at 90 ºC (363 K), which was ~12 % compared with the IT of 40ºC (313 K), which was not plotted in Fig. 5.

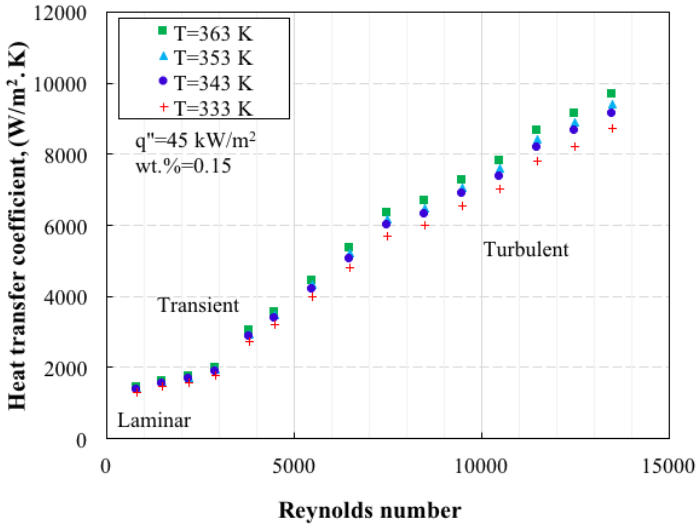

Figure 5. Effect of Re number on the HTC value of the NF.

Pressure drop

In Figure 6, the effect of the flow on the pressure drop (PD) value of the system. As shown, with increasing the flow rate, the PD value non-linearly increased. Also, the presence of the NPs increased the PD of the system. At Reynolds number of 1500, the PD value of water and NF at wt.% of 0.15 was 2.6 kPa and 3.6 kPa, while at Re=13500, the PD for water and NF reached 6.8 kPa and 9.6 kPa. It represents that the PD of the system is augmented. This augmentation can be attributed to the enhancement in the viscosity of the base fluid. The presence of the NPs added frictional forces into the layer-layer interfaces. It also increased the collision and the friction between particle-particle interfaces, which directly influenced the viscosity of the NF. Also, the PD of the system in the laminar region was the lowest and the highest PD value was obtained for the turbulent region.

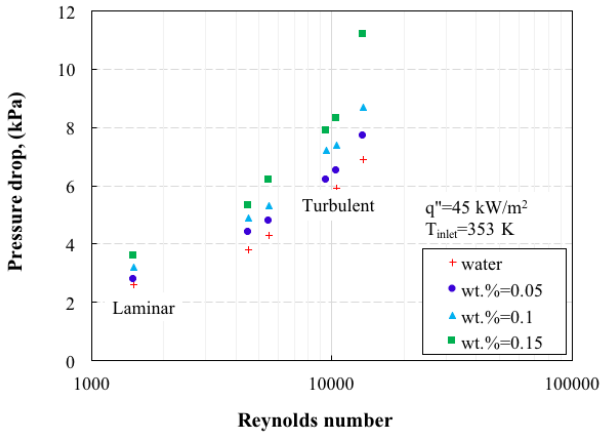

Figure 6. Effect of the Reynolds number on the PD value.

Nanoparticle fouling

Figure 7 represents the dependence of the HTC on the time of the experiments for NF at wt.% of 0.1 and HF of 45 kW/m^2. As can be seen, within the first 60 minutes of the experiments, the HTC showed a steady behaviour with time, however, over a period of 1000 minutes of the operation, the HTC slightly decreased. This is because, with time, the rate of deposition for NPs increased such that a continual but a porous layer of NPs form on the heating surface. This layer not only filled the irregularities and micro-cavities of the surface but also created a thermal resistance on the heating surface. Such thermal resistance can decrease the HTC and in addition to this, the porous layer suppressed the bubble formation as well. Hence, with time, the thickness of the deposition increased and the bubble formation was deteriorated. That being said, the HTC decreased over time. The fouling thermal resistance (FTR) of the system at wt.%=0.15 reached > 0.06 m^2. K/kW after 1000 minutes of experiments. As perceived, the reduction of heat transfer showed a rectilinear trend similar to the FTR. Notably, 1000 minutes of operation was a standard for investigating the fouling and transient experiments on sub-micron particles [10].

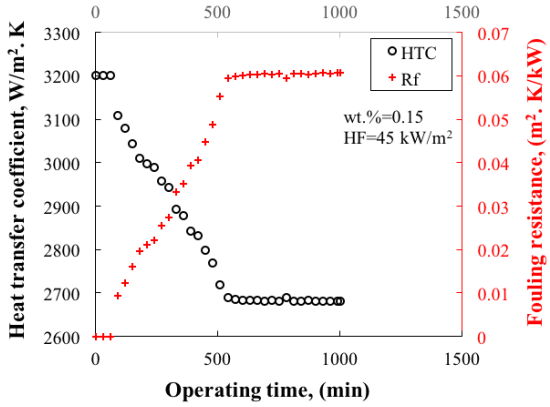

Figure 7. Variation of the HTC and FTR with time for 1000 minutes of the operation.

In Figure 8. The fouling resistance trend against time is depicted for different NFs. As perceived, the FTR parameter increased with time-spanning reaching a maximum value under an asymptotic trend. Also, with

increasing the concentration, the FTR of the system slightly increased. This is because, at larger mass concentrations, more particles deposited on the surface creating a thick sedimentation layer. The layer decreased the HTC by increasing the thermal resistance and also due to the suppression of the bubble formation. As mentioned before, the bubble formation was under the influence of surface characteristics, meaning that for a smooth surface, the bubble formation rate can be lower than that of observed for a rough and surfaces with irregularities. Hence, with an increase in the mass concentrations of NF, the bubble formation decreased over time resulting in the reduction in the HTC of the system. Noticeably, at first minutes of the experiments, bubble formation hindered the formation of deposition on the surface, however, with time, a small layer of particle formed on the surface, which increased the stick-ability of the surface. Therefore, more NPs attached to the fouling layer, which increased the FTR. Such fouling layer, due to the porosity and the capture of vapour in the porous layer, decreased the conductivity of the surface as well. Hence, HTC decreased with time. The maximum FTR of the system was 0.053. 0.058 and 0.064 m^2. K/kW for wt.%=0.05, 0.1 and 0.15, respectively.

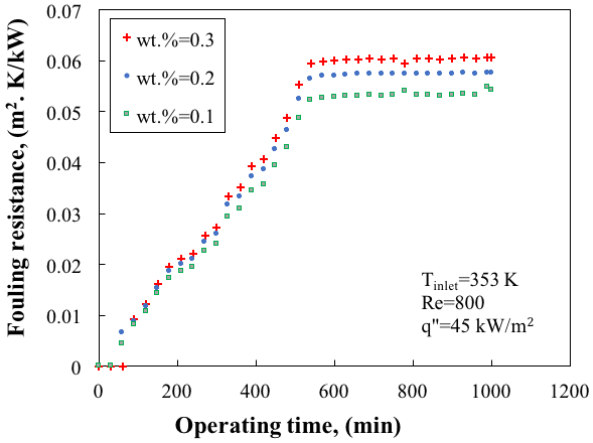

Figure 8. Variation of the FTR with time for different NFs.

Figure 9a represents a comparison chart between the resistance values extracted from the literature and those calculated from the experiments [58]. As perceived, the calculated data are in a reasonable agreement with those of data extracted from the literature within the deviation of ±20%. This was because the comparison was made between the fouling resistance measured in the NF and the FTR in the micro-fluids. Hence, due to the significant difference between the micro-fluids and NFs, the thermal fouling resistance was also different. Please note that the thickness of the fouling for the micro-fluids was larger than that of observed for the NFs. As can also be seen in Fig. 9b, results of the comparison between the HTC measured for water and the HTC calculated with the Chen model [59] showed that the experimental data were in a good agreement with Chen model within the deviation of ±4% and ±7%, respectively. Therefore, FTR obtained with the experiments and also the HTC measured with the test rig are reliable.

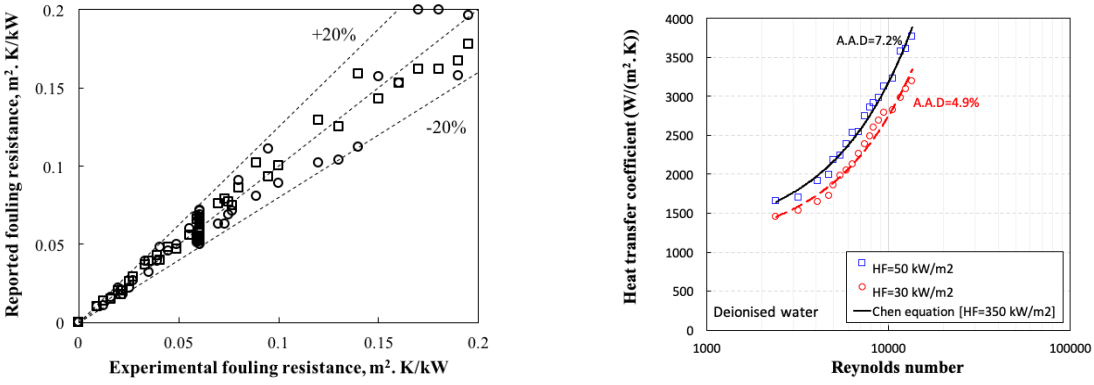

Figure 9. (a) The comparison chart of the reported FTR and those measured by the experiments and (b) the measured HTC against those of calculated with Chen correlation.

Figure 10 represents the boiling surface before and after 300 and 1000 minutes of the boiling tests with NF at wt.%=0.15. As can be seen, the roughness of the boiling surface vanished over time and a porous layer formed on the surface. However, for the clean surface, the roughness can provide sufficient extended area for the bubbles to form, grow and detach. Overall, titanium oxide/deionized water showed a great thermal performance in the forced convective heat transfer domain, however, it did not provide plausible heat transfer characteristics over the extended operating time due to the massive deposition of NPs on the surface. The images have been taken with Digi-scope IDP 200X.

(a) clean surface (b) after 300 min (c) after 1000 min

Figure 10. The visualization of the surface before and after the boiling experiments with NFs.

Bubble interaction

In Figure 11, bubble formation and the effect of the AHF on the rate of formation is depicted. As shown, with increasing the AHF, the mechanism for the generation of the bubble is somehow fortified, and due to the enhanced evaporation, bigger bubbles are seen. At HF 25 kW/m^2, the bubbles were relatively small in comparison with other AHFs. However, with increasing the HF, layers of fluid become agitated and more local movements were observed close to the heating surface. As a result of such movements, bubbles were merged and the size of the bubbles become larger. Also, as a result of such movements, some micro-convective streams are formed which locally increase the HTC value. Thus, at higher HFs, larger bubbles, higher movements and larger HTC was observed. Also, the mean bubble size for the case of NF was relatively larger than those measured for the pure water. This was because the presence of the NPs increases the bubble detaching time resulting in the augmentation in the mean residence time recorded for each bubble on the heating surface. Hence, bubbles have more time to grow on the surface, which results in the production of the larger bubbles. Also, NPs can change the size of the irregularities, which in turn creates larger bubbles at the onset of nucleate boiling. Hence, larger bubbles were seen for the case of NFs.

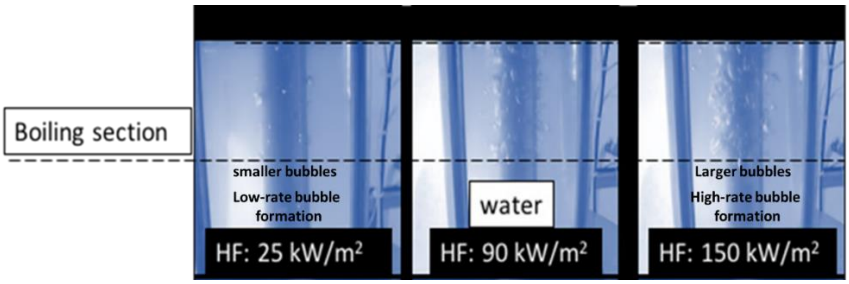

Figure 11. Bubble formation of the NF at various HFs.

CONCLUDING REMARKS

Following concluding remarks were obtained by assessing the experimental results:

(1) HF and flow rate of NF enhanced the mean value of the HTC. It was perceived that amount of augmentation in HTC pertaining to HF was larger than that does record for the other parameters. Two pivotal heat transfer mechanisms of forced convective and nucleate boiling were found as the dominant governing heat transfer mode.

(2) The presence of titanium oxide NPs enhanced HTC. This was justified based on the enhancement in micro- and nano-scale phenomena such as random Brownian motion and also a surface-liquid thermophoresis effect.

Also, the augmentation of the thermal conductivity was another major parameter for enhancing the HTC value. The maximum enhancement in the HTC was 34% at wt.% of 0.15 and the calculated Reynolds number of ~13500.

(3) The quantified PD was also augmented with increasing the wt.% of the NPs. The highest recorded PD was 9 kPa at wt.%=0.15 and Re=13500, which was 28% larger than that of measured for the base fluid.

(4) HTC and PD had a trade-off behaviour. Hence, more experiments are highly recommended to identify the operating conditions in which the PD is minimized, while the enhancement in HTC is maximized.

(5) The formation of fouling on the heating surface over the 1000 minutes of experiments showed that the HTC of the NF may drop by 21.6% due to the thermal resistance induced by the fouling layer.

REFERENCES

[1] Stephan K, Abdelsalam M. Heat-transfer correlations for natural convection boiling. Int J Heat Mass Trans 1980; 23:73-87. DOI: 10.1016/0017-9310(80)90140-4.

[2] Madani K. Numerical investigation of cooling a ribbed microchannel using nanofluid. J Therm Eng 2018;4(6):2408-22. DOI: 10.18186/thermal.465650.

[3] Vassallo P, Kumar R, D'Amico S. Pool boiling heat transfer experiments in silica–water nano-fluids. Int J Heat Mass Trans 2004;47(2):407-11. DOI: 10.1016/S0017-9310(03)00361-2.

[4] Lazarek G, Black S. Evaporative heat transfer, pressure drop and critical heat flux in a small vertical tube with R-113. Int J Heat Mass Trans 1982;25(7):945-60. DOI: 10.1016/0017-9310(82)90070-9.

[5] Zahmatkesh I. Effect of magnetic field orientation on nanofluid free convection in a porous cavity: a heat visualization study. J Therm Eng 2020;6(1):170-86. DOI: 10.18186/thermal.672297.

[6] Almakki M, Mondal H, Sibanda P. Entropy generation in MHD flow of viscoelastic nanofluids with homogeneous-heterogeneous reaction, partial slip and nonlinear thermal radiation. J Therm Eng 2020;6(3):327-45. DOI: 10.18186/thermal.712452.

[7] Liang G, Mudawar I. Review of pool boiling enhancement with additives and nanofluids. Int. J. Heat Mass Trans 2018; 124:423-53. DOI: 10.1016/j.ijheatmasstransfer.2018.03.046

[8] Lazarus G, Roy S, Kunhappan D, Cephas E, Wongwises S. Heat transfer performance of silver/water nanofluid in a solar flat-plate collector. J Therm Eng 2015;1(2):104-12. DOI: 10.18186/jte.29475.

[9] Sarafraz M. Experimental investigation on pool boiling heat transfer to formic acid, propanol and 2-butanol pure liquids under the atmospheric pressure. J Appl Fluid Mech 20136(1):73-79. DOI: 10.36884/jafm.6.01.19494.

[10] Sarafraz M, Nikkhah V, Nakhjavani M, Arya A. Fouling formation and thermal performance of aqueous carbon nanotube nanofluid in a heat sink with rectangular parallel microchannel. App Therm Eng 2017; 123:29-39. DOI: 10.1016/j.applthermaleng.2017.05.056.

[11] Sarafraz M, Peyghambarzadeh S, Alavifazel S. Enhancement of nucleate pool boiling heat transfer to dilute binary mixtures using endothermic chemical reactions around the smoothed horizontal cylinder. Heat Mass Trans 2012;48(10):1755-65. DOI: 10.1007/s00231-012-1019-5.

[12] Drummond KP, Back D, Sinanis MD, Janes DB, Peroulis D, Weibel JA, et al. A hierarchical manifold microchannel heat sink array for high-heat-flux two-phase cooling of electronics. Int J Heat Mass Trans 2018; 117:319-30. DOI: 10.1016/j.ijheatmasstransfer.2017.10.015.

[13] Sarafraz MM, Pourmehran O, Yang B, Arjomandi M, Ellahi R. Pool boiling heat transfer characteristics of iron oxide nano-suspension under constant magnetic field. Int J Therm Sci 2020; 147:106131. DOI: 10.1016/j.ijthermalsci.2019.106131.

[14] Sarafraz MM, Peyghambarzadeh SM. Nucleate pool boiling heat transfer to Al2O3-water and TiO2-water nanofluids on horizontal smooth tubes with dissimilar homogeneous materials. Chem Biochem Eng Q 2012;26(3):199-206. DOI: 10.15255/CABEQ.2014.127.

[15] Arya A, Sarafraz M, Shahmiri S, Madani S, Nikkhah V, Nakhjavani S. Thermal performance analysis of a flat heat pipe working with carbon nanotube-water nanofluid for cooling of a high heat flux heater. Heat Mass Trans 2018;54(4):985-97. DOI: 10.1016/j.ijheatmasstransfer.2012.06.086.

[16] Nakhjavani M, Nikkhah V, Sarafraz M, Shoja S, Sarafraz M. Green synthesis of silver nanoparticles using green tea leaves: Experimental study on the morphological, rheological and antibacterial behaviour. Heat Mass Trans 2017;53(10):3201-9. DOI: 10.1007/s00231-017-2065-9.

[17] Nikkhah V, Sarafraz M, Hormozi F. Application of spherical copper oxide (II) water nano-fluid as a potential coolant in a boiling annular heat exchanger. Chem Biochem Eng Q 2015;29(3):405-15. DOI: 10.15255/CABEQ.2014.2069.

[18] Peyghambarzadeh S, Sarafraz M, Vaeli N, Ameri E, Vatani A, Jamialahmadi M. Forced convective and subcooled flow boiling heat transfer to pure water and n-heptane in an annular heat exchanger. Annals Nuc Ene 2013; 53:401-10. DOI: 10.1016/j.anucene.2012.07.037.

[19] Salari E, Peyghambarzadeh S, Sarafraz M, Hormozi F, Nikkhah V. Thermal behavior of aqueous iron oxide nano-fluid as a coolant on a flat disc heater under the pool boiling condition. Heat Mass Transfer 2017;53(1):265-75. DOI: 10.1007/s00231-016-1823-4.
[20] Kamel MS, Lezsovits F, Hussein AM, Mahian O, Wongwises S. Latest developments in boiling critical heat flux using nanofluids: A concise review. Int Commun Heat Mass Trans 2018; 98:59-66. DOI: 10.1016/j.icheatmasstransfer.2018.08.009.
[21] Bhattad A, Sarkar J, Ghosh P. Improving the performance of refrigeration systems by using nanofluids: A comprehensive review. Rene Sus Ene Rev 2018; 82:3656-69. DOI: 10.1016/j.rser.2017.10.097.
[22] Parlak N. Experimental validation of LMTD method for microscale heat transfer. J Therm Eng 2017;3(2):1181-95. DOI: 10.18186/thermal.298619.
[23] Sharma B. Effect of flow structure on heat transfer in compact heat exchanger by using finite thickness winglet at acute angle. J Therm Eng 2017;3(2):1149-62. DOI: 10.18186/thermal.298616.
[24] Belhadj A. Numerical investigation on of forced convection of nanofluid in microchannels heat sinks. J Therm Eng 2018;4(5):2263-73. DOI: 10.18186/thermal.438480.
[25] Akinshilo A, Ilegbusi AO. Investigation of Lorentz force effect on steady nanofluid flow and heat transfer through parallel plates. J Thermal Eng. 2019; 5:482-97. DOI: 10.18186/thermal.625919.
[26] Bayareh M. Numerical simulation and analysis of heat transfer for different geometries of corrugated tubes in a double pipe heat exchanger. J Therm Eng 2019;5(4):293-301. DOI: 10.18186/thermal.581775.
[27] Ekiciler R, Aydeniz E, Arslan K. A CFD investigation of al2o3/water flow in a duct having backward-facing step. J Therm Eng 2019;5(1):31-41. DOI: 10.18186/thermal.512999.
[28] Ravisankar R, Venkatachalapathy VSK, Alagumurthi N. Application of nanotechnology to improve the performance of tractor radiator using cu-water nanofluid. J Therm Eng 2018;4(4):2188-200. DOI: 10.18186/journal-of-thermal-engineering.434036.
[29] Han D, He W, Asif F. Experimental study of heat transfer enhancement using nanofluid in double tube heat exchanger. Energy Procedia. 2017; 142:2547-53. DOI: 10.1016/j.egypro.2017.12.090.
[30] Ali HM, Babar H, Shah TR, Sajid MU, Qasim MA, Javed S. Preparation techniques of TiO2 nanofluids and challenges: a review. Appl Sci 2018;8(4):587. DOI: /10.3390/app8040587.
[31] Vakili M, Mohebbi A, Hashemipour H. Experimental study on convective heat transfer of TiO2 nanofluids. Heat Mass Transfer 2013;49(8):1159-65. DOI: /10.1016/j.icheatmasstransfer.2012.01.004.
[32] Azmi W, Hamid KA, Usri N, Mamat R, Mohamad M. Heat transfer and friction factor of water and ethylene glycol mixture based TiO2 and Al2O3 nanofluids under turbulent flow. INT COMMUN HEAT MASS 2016; 76:24-32. DOI: 10.1016/j.icheatmasstransfer.2016.05.010
[33] Karthikeyan A, Coulombe S, Kietzig A. Boiling heat transfer enhancement with stable nanofluids and laser textured copper surfaces. Int J Heat Mass Transf 2018; 126:287-96. DOI: 10.1016/j.ijheatmasstransfer.2018.05.118.
[34] Sarafraz M, Arya A, Nikkhah V, Hormozi F. Thermal performance and viscosity of biologically produced silver/coconut oil Nanofluids. Chem Biochem Eng Q 2017;30(4):489-500. DOI: 10.15255/CABEQ.2015.2203.
[35] Sarafraz M, Hormozi F. Application of thermodynamic models to estimating the convective flow boiling heat transfer coefficient of mixtures. Exp Therm Fluid Sci 2014; 53:70-85. DOI: 10.1016/j.expthermflusci.2013.11.004.
[36] Sarafraz M, Hormozi F, Kamalgharibi M. Sedimentation and convective boiling heat transfer of CuO-water/ethylene glycol nanofluids. Heat Mass Transfer 2014;50(9):1237-49. DOI: 10.1007/s00231-014-1336-y.
[37] Sarafraz M, Hormozi F, Peyghambarzadeh S, Vaeli N. Upward Flow Boiling to DI-Water and Cuo Nanofluids Inside the Concentric Annuli. J Appl Fluid Mech J APPL FLUID MECH 2015;8(4). DOI: 10.18869/acadpub.jafm.67.223.19404.
[38] Sarafraz M, Nikkhah V, Nakhjavani M, Arya A. Thermal performance of a heat sink microchannel working with biologically produced silver-water nanofluid: experimental assessment. Exp Therm Fluid Sci 2018; 91:509-19. DOI: 10.1016/j.expthermflusci.2017.11.007.
[39] Aouanouk AS. Numerical study of milk fouling thickness in the channel of plate heat exchanger. J Therm Eng 2018;4(6):2464-70. DOI: 10.18186/thermal.465692.
[40] Sarafraz M, Arjomandi M. Demonstration of plausible application of gallium nano-suspension in microchannel solar thermal receiver: Experimental assessment of thermo-hydraulic performance of microchannel. INT COMMUN HEAT MASS 2018; 94:39-46. DOI: 10.1016/j.icheatmasstransfer.2018.03.013.
[41] Sarafraz M, Arjomandi M. Thermal performance analysis of a microchannel heat sink cooling with Copper Oxide-Indium (CuO/In) nano-suspensions at high-temperatures. Appl Therm Eng 2018; 137:700-9. DOI: 10.1016/j.applthermaleng.2018.04.024.
[42] Sarafraz M, Arya H, Arjomandi M. Thermal and hydraulic analysis of a rectangular microchannel with gallium-copper oxide nano-suspension. J Mol Liq 2018; 263:382-9. DOI: 10.1016/j.molliq.2018.05.026.
[43] Tong LS. Boiling heat transfer and two-phase flow: Routledge; 2018.

[44] Alhashan T, Addali A, Teixeira JA, Naid A. Experimental investigation of the influences of different liquid types on acoustic emission energy levels during the bubble formation process. Int J Energy Environ Eng 2018;9(1):13-20. DOI: 10.1007/s40095-017-0245-5.
[45] Babu RV, Verma KA, Charan M, Kanagaraj S. Tweaking the diameter and concentration of carbon nanotubes and sintering duration in Copper based composites for heat transfer applications. Adv Powder Technol 2018;20(10):2356-67. DOI: 10.1016/j.apt.2018.06.015.
[46] Huang D, Wu Z, Sunden B. Effects of hybrid nanofluid mixture in plate heat exchangers. Exp Therm Fluid Sci 2016; 72:190-6. DOI: 10.1016/j.expthermflusci.2015.11.009.
[47] Sarafraz M, Peyghambarzadeh S. Influence of thermodynamic models on the prediction of pool boiling heat transfer coefficient of dilute binary mixtures. INT COMMUN HEAT MASS 2012;39(8):1303-10. DOI: 10.1016/j.icheatmasstransfer.2012.06.020.
[48] Sarafraz MM, Peyghambarzadeh SM. Experimental study on subcooled flow boiling heat transfer to water–diethylene glycol mixtures as a coolant inside a vertical annulus. Exp Therm Fluid Sci 2013; 50:154-62. DOI: 10.1016/j.expthermflusci.2013.06.003.
[49] Nikkhah V, Sarafraz MM, Hormozi F, Peyghambarzadeh SM. Particulate fouling of CuO–water nanofluid at isothermal diffusive condition inside the conventional heat exchanger-experimental and modeling. Exp Therm Fluid Sci 2015; 60:83-95. DOI: 10.1016/j.expthermflusci.2014.08.009
[50] Kline S, McClintock F. Jan., 1953," Describing the uncertainties in experimental results". Exp Therm Fluid Sci 1988; 1:3-17. DOI: 10.1016/0894-1777(88)90043-X.
[51] Sarafraz M, Peyghambarzadeh S, Alavi Fazel S, Vaeli N. Nucleate pool boiling heat transfer of binary nano mixtures under atmospheric pressure around a smooth horizontal cylinder. Period. Polytech Chem Eng 2013;57(1-2):71-7. DOI: 10.3311/PPch.2173.
[52] Sarafraz M, Peyghambarzadeh S, Vaeli N. Subcooled flow boiling heat transfer of ethanol aqueous solutions in vertical annulus space. Chem Ind Chem Eng Q 2012;18(2):315-27. DOI: 10.2298/CICEQ111020008S.
[53] Sarafraz MM, Hormozi F. Forced convective and nucleate flow boiling heat transfer to alumnia nanofluids. Period Polytech Chem Eng 2014;58(1):37-46. DOI: 10.3311/PPch.2206.
[54] Sarafraz M, Arya A, Hormozi F, Nikkhah V. On the convective thermal performance of a CPU cooler working with liquid gallium and CuO/water nanofluid: A comparative study. Appl Therm Eng 2017; 112:1373-81. DOI: 10.1016/j.applthermaleng.2016.10.196.
[55] Sarafraz M, Arya H, Saeedi M, Ahmadi D. Flow boiling heat transfer to MgO-therminol 66 heat transfer fluid: Experimental assessment and correlation development. Appl Therm Eng 2018;138:552-62. DOI: 10.1016/j.applthermaleng.2018.04.075.
[56] Sarafraz M, Hart J, Shrestha E, Arya H, Arjomandi M. Experimental thermal energy assessment of a liquid metal eutectic in a microchannel heat exchanger equipped with a (10 Hz/50 Hz) resonator. Appl Therm Eng 2019; 148:578-90. DOI: 10.1016/j.applthermaleng.2018.11.073.
[57] Hocaoglu S, Ozkan DB. The effect of system parameters on the condensation performance of heat pump system using R290. J Therm Eng 2018;4(5):2248-62. DOI: 10.18186/journal-of-thermal-engineering.436137.
[58] Peyghambarzadeh S, Vatani A, Jamialahmadi M. Experimental study of micro-particle fouling under forced convective heat transfer. Braz J Chem Eng 2012;29(4):713-24. DOI: 10.1590/S0104-66322012000400004.
[59] Huo X, Chen L, Tian Y, Karayiannis T. Flow boiling and flow regimes in small diameter tubes. Appl Therm Eng 2004;24(8-9):1225-39. DOI: 10.1016/j.applthermaleng.2003.11.027